ISSN 2075-1087, Gyroscopy and Navigation, 2025, Vol. 16, No.2, pp. 110–121
Original Russian Text A.V. Fomichev published in Giroskopiya i Navigatsiya, 2025, Vol. 33, No. 2, pp. 3–20

Estimation and Compensation of Strapdown Inertial Navigation System Errors Caused by Inertial Sensor Delays

A.V. Fomichev

Moscow Institute of Electromechanics and Automatics, Moscow, Russia
e-mail: a.fomichev@aomiea.ru
Received: December 5, 2024; revised: April 19, 2025; accepted: July 9, 2025

Abstract: The paper discusses how the data delays of inertial sensors within a strapdown inertial navigation system affect the accumulation of inertial navigation errors. The vehicle motions when this effect is particularly significant are identified in operation and ground-based experiments. Recommendations on delay estimation and further algorithmic compensation are provided.

Key words: strapdown inertial navigation system (SINS), delays in the inertial sensor measurements, navigation accuracy, delays estimation and compensation

INTRODUCTION

The accuracy of SINS depends on inertial sensor instrumental errors and on numerical algorithms of integrating the SINS differential equations. These issues have been covered in abundant literature (see, for instance, [1–10] and many other publications). Another important factor for SINS accuracy is the proper synchronization of measurements from inertial sensors: accelerometers and angular rate sensors (ARS), or gyroscopes [11–18], and for aided SINS, synchronization of aiding data and SINS autonomous solution [19–24].

The paper analyzes the effect of delays in inertial sensor measurements – time intervals between the data readout and its input to the navigation algorithm – on SINS accuracy. These delays may be caused by SINS hardware features, raw sensor data processing methods, lags during data transmission by communication lines and real-time filtering.

The influence of delays on the SINS accuracy depends on the object trajectory: under intensive maneuvering, vibration, or oscillations even small delays may critically affect the SINS accuracy.

Further we consider the inertial sensor delays to be stable, which is conditioned by the rather strict cyclogram of SINS hardware operation. This model helps to determine the level and evolution of the navigation errors and obtain some analytical estimates.

The main objectives of this study, which define its structure, are given below:

- to obtain the disturbing components for the sensor delays in the right sides of SINS error linear differential equations, which are known to well describe the time evolution of errors for rather accurate SINS [1–3];
- to identify SINS case angular motions, which are easily reproducible in laboratory experiments, that can be used to detect and estimate the delays by the output errors in SINS inertial data, and, on the other side, to explain the evolution of the latter;
- for the maneuvers short as compared to the Schuler period, to obtain the analytical expressions to estimate the delay impact under arbitrary angular motion in laboratory experiments, when the measurement center of the accelerometer unit can be considered stationary;
- to analyze, based on these expressions, how the delays in accelerometer, gyroscope data, and between the axes of one type sensors influence the navigation errors, and to propose delay algorithmic compensation.

Along with this, the paper supplements, generalizes, and systematizes the findings obtained in [11–18].

MODEL OF INERTIAL SENSOR DATA DELAYS

The SINS sensitive elements are the accelerometers and angular rate sensors, or gyroscopes. The accelerometers measure the specific force $f = w - g$ projected on their sensitivity axes, where w is the sensor absolute acceleration, and g is the specific gravity force. The gyroscopes measure the projection of the absolute angular rate ω on their sensitivity axes. Here we assume that the sensors measure the instantaneous values of f and ω, however, discussions will be true for integrating sensors, too.

As a rule, the sensors sensitivity axes are structurally or algorithmically aligned with the axes of some orthogonal trihedral p, referred to as the SINS frame. We take the sensitivity axes of sensors and trihedral p to be codirectional.

Denote the measurement delay for the i-th axis of accelerometer channel by $\tau_i^a = \text{const}$, and for the i-th axis of gyroscope channel, by $\tau_i^g = \text{const}$. The readings of accelerometer unit f_p' and gyroscope unit ω_p' in the SINS frame p are described with the following models:

$$f_p'(t) = \begin{bmatrix} f_{p_1}(t-\tau_1^a) \\ f_{p_2}(t-\tau_2^a) \\ f_{p_3}(t-\tau_3^a) \end{bmatrix} \approx f_p(t) - \begin{bmatrix} \dot f_{p_1}(t)\tau_1^a \\ \dot f_{p_2}(t)\tau_2^a \\ \dot f_{p_3}(t)\tau_3^a \end{bmatrix},$$
$$\omega_p'(t) = \begin{bmatrix} \omega_{p_1}(t-\tau_1^g) \\ \omega_{p_2}(t-\tau_2^g) \\ \omega_{p_3}(t-\tau_3^g) \end{bmatrix} \approx \omega_p(t) - \begin{bmatrix} \dot\omega_{p_1}(t)\tau_1^g \\ \dot\omega_{p_2}(t)\tau_2^g \\ \dot\omega_{p_3}(t)\tau_3^g \end{bmatrix}. \quad (1)$$

Here f_p and ω_p are the physical values of specific force and angular rate, t is the current time; lower index of any vector here and below denotes the coordinate frame, and decompositions are made on the assumption of delay smallness.

Along with the delay-induced errors, the sensor measurements contain other errors such as due to bias and scale factor errors. However, linear system of SINS error equations allows analyzing the partial contribution of each navigation error source separately, so further we focus only on the model of the delay-induced error (1).

The formulas (1) provide compact index and vector-matrix notations of the sensor errors $\Delta f_p^\tau = f_p' - f_p$ and $\nu_p^\tau = \omega_p' - \omega_p$:

$$\Delta f_{p_i}^\tau = -\tau_i^a \dot f_{p_i},\ \ \nu_{p_i}^\tau = -\tau_i^a \dot\omega_{p_i} \ \Leftrightarrow$$
$$\Leftrightarrow \Delta f_{p_i}^\tau = -T^a \dot f_p,\ \nu_p^\tau = -T^g \dot\omega_p, \quad (2)$$

where $T^a = \text{diag}[\tau_i^a], T^g = \text{diag}[\tau_i^g]$. Since the right part of Eqs. (2) are proportional to the derivatives $\dot f_p, \dot\omega_p$, data delay in the sensor channels is manifested during the object maneuvering, when the measured specific force and angular rate greatly change with time.

DELAY EFFECT ON SINS NAVIGATION ERRORS

The SINS errors are described with a system of linear differential equations [1–3], which have the following form in the wander azimuth navigation frame:

$$\begin{aligned}
\Delta\dot r_1 &= \delta V_1 + \beta_3 V_2' - \left(\alpha_2 - \frac{\Delta r_1}{a}\right) V_3' + \Omega_3' \Delta r_2, \\
\Delta\dot r_2 &= \delta V_2 - \beta_3 V_1' + \left(\alpha_1 + \frac{\Delta r_2}{a}\right) V_3' - \Omega_3' \Delta r_1, \\
\delta\dot V_1 &= -g\alpha_2 + (\Omega_3' + 2u_3')\delta V_2 - (\Omega_2' + 2u_2')\delta V_3 + \Delta f_1, \\
\delta\dot V_2 &= g\alpha_1 - (\Omega_3' + 2u_3')\delta V_1 + (\Omega_1' + 2u_1')\delta V_3 + \Delta f_2, \quad (3) \\
\dot\alpha_1 &= -\frac{\delta V_2}{a} + \omega_3'\alpha_2 - u_2'\beta_3 - u_3'\frac{\Delta r_1}{a} + \nu_1, \\
\dot\alpha_2 &= \frac{\delta V_1}{a} - \omega_3'\alpha_1 + u_1'\beta_3 - u_3'\frac{\Delta r_2}{a} + \nu_2, \\
\dot\beta_3 &= \omega_3'\left(\alpha_1 + \frac{\Delta r_2}{a}\right) - \omega_1'\left(\alpha_2 - \frac{\Delta r_1}{a}\right) + \nu_3,
\end{aligned}$$

where indices 1, 2, 3 denote the vector component along the axis of trihedral y – the image of reference geographical trihedral x calculated by SINS [1–3];

Δr_i are the positioning errors;

δV_i are the velocity dynamic errors [1–3];

α_i are the vertical dynamic errors;

β_3 is the azimuth kinematic error;

a is the Earth's equatorial radius;

Δf_i are the overall errors of accelerometer channel projected on the axes of trihedral y;

ν_i are the overall errors of gyroscope channel projected on the axes of trihedral y, the prime sign «′» denotes the parameters calculated in the navigation system;

V_i' are the components of the vector of linear velocity with respect to the Earth in trihedral y;

Ω'_i are the components of the angular rate vector of the model reference trihedral *y*;

u'_i are the components of the Earth's angular rate vector in trihedral *y*;

ω'_i are the components of the absolute angular rate vector of trihedral *y* in its axes.

The overall errors in the SINS trihedral *p* are the differences between the measured sensor signals and the physical values that could be measured by ideal sensors installed on the orthogonal axes of trihedral *p*. For gyroscopes, $\nu_p = \omega'_p - \omega_p$, where ω'_p is the measured angular rate ω_p. Similarly, for accelerometers $\Delta f_p = f'_p - f_p$, where f'_p and f_p are the measured accelerometer signals and the physical values of specific force, respectively. Thus, the values Δf_i and ν_i in the right part of (3) are formed by reprojecting Δf_p and ν_p onto the trihedral *y*:

$$\Delta f_y = D'_{zp}\Delta f_p, \quad \nu_y = -D'_{zp}\nu_p, \tag{4}$$

using the matrix D'_{zp} calculated by SINS and relating the SINS trihedral *p* with the quasiinstrument trihedral *z*, which is the image of the platform trihedral for SINS. For more detailed description of these trihedral, the reader is referred to [1–3].

Formulas (3)-(4) can be used to analyze the influence of an arbitrary combination of delays at any trajectory. Rewrite the system (3) in vector-matrix form:

$$\dot{x} = Ax + \delta^\tau, \tag{5}$$

where $x = [\Delta r_1, \Delta r_2, \delta V_1, \delta V_2, \alpha_1, \alpha_2, \beta_3]^T$ is the state vector of system (3); *A* is its matrix; δ^τ are the delay-induced instrumental errors for the delays

$$\Delta f_y^\tau = D'_{zp}\Delta f_p^\tau, \quad \nu_y^\tau = -D'_{zp}\nu_p^\tau, \tag{6}$$

where Δf_p^τ, ν_p^τ are found using (2). The system (5) is integrated with initial conditions $x(0) = 0$ to obtain the solution $x(t)$ corresponding to the delays.

ANALYTICAL ESTIMATIONS OF NAVIGATION ERRORS UNDER SHORT MANEUVERS AS COMPARED TO THE SCHULER PERIOD

As is known, the SINS error equations system (3) has a typical Schuler period T_0 = 84.4 minutes. Thus, Δf_y, ν_y in the right side of (3) can be classified as fast or slow by comparing with T_0. From this viewpoint, the maneuvers during operation and laboratory experiments are mostly short, i.e., fast.

For a fast maneuver, the vectors of delay-induced errors (6) are assumed impulse functions. For them, the increments in components of the state vector in the error equations system (3) during the maneuver can be calculated approximately avoiding precise integration. This qualitatively explains some effects observed in the experiments and helps to obtain analytical expressions relating the navigation errors and delays in sensor measurements. The estimation accuracy depends on the maneuver duration and can be evaluated by comparing with the numerical solution of equations (5) if required.

It is known that SINS with 1 nm/h positioning error features accelerometer biases $\Delta f \sim 10^{-3}$ m/s^2 and gyroscope drifts $\nu \sim 10^{-2}$ deg/h, where ~ denotes the order of the magnitude. Further we estimate the order of delay-induced errors with these typical values.

If the vector f_p is set in moving frame *p* with angular rate ω_p, from theoretical mechanics we know its absolute derivative $df_p/dt = \dot{f}_p + \omega_p \times f_p$ [25–28], where the dotted character is the vector local derivative formed by the derivatives of each vector component with time. If all formula terms are considered to have the same order, then $|\dot{f}_p| \sim |\omega_p||f_p|$. For the angular rate vector $\omega_p \times \omega_p = 0$ and $d\omega_p/dt = \dot{\omega}_p$. Also note that under instantaneous mechanical action on SINS f_p also changes instantaneously and at this moment $|\dot{f}_p| \to \infty$, however, the applied forces are actually changing continuously, so we take $|\dot{f}_p| \sim |\omega_p||f_p|$. Hence,

$$|\Delta f_p^\tau| \sim \tau^a |\dot{f}_p| \sim \tau^a |\omega_p||f_p|, \ |\nu_p^\tau| \sim \tau^g |\dot{\omega}_p|.$$

Consider a case with sensor delays of the order $\tau^i \sim 10^{-3}$ s with motion parameters $|f_p| \sim 50$ m/s^2, $|\omega_p| \sim 60$ deg/s, $|\dot{\omega}_p| \sim 200$ deg/s^2, which are quite typical, for example, for an airborne SINS.

Then $|\Delta f_p^\tau| \sim 10^{-2}$ m/s^2, $|\nu_p| \sim 0.1$ deg/h. Hence it is seen that the error due to the delays $\tau^i \sim 10^{-3}$ s may be an order higher than the typical instrumental errors of a 1 nm/h grade SINS.

Accelerometer impulse errors are denoted with Δf_1, Δf_2 in the right side of system (3). It can be noted that within their action period *T* only the dynamic velocity errors δV_i change significantly, and the other components of the state vector (3) vary slightly. This can be checked using the estimates of

the right sides of the error equations and by modeling. Thus, the increments of velocity dynamic errors are given by the formulas:

$$\delta V_1(T) \approx \int_0^T \Delta f_1^\tau(t)dt,\ \delta V_2(T) \approx \int_0^T \Delta f_2^\tau(t)dt. \quad (7)$$

Consider the impact of gyro impulse drifts on the navigation errors. Recall that in the theory of inertial navigation the angular errors are divided into dynamic and kinematic ones [1–3]. The kinematic error is characterized by the small rotation vector β, which, in its turn, is conditioned by the initial alignment errors of SINS and gyroscopes, including the drifts due to delays. The vector β_y in trihedral y satisfies to the kinematic error equations:

$$\dot\beta_y = \hat\omega'_y\beta_y + \nu_y,\ \hat\omega'_y = \begin{bmatrix} 0 & \omega'_3 & -\omega'_2 \\ -\omega'_3 & 0 & \omega'_1 \\ \omega'_2 & -\omega'_1 & 0 \end{bmatrix}. \quad (8)$$

Here and below the superscript «^» denotes the operator of the left vector multiplication with inverse sign, for example, $\hat\omega'_y\beta_y = -\omega'_y \times \beta_y$; ν_y is the gyroscope overall drift.

The linearity of (8) helps to study the partial contribution of gyroscope data delay β_y^τ described as

$$\dot\beta_y^\tau = \hat\omega'_y\beta_y^\tau + \nu_y^\tau,\ \ \beta_y^\tau(0) = 0.$$

The angular rate ω'_y of trihedral y is commensurate with the Earth's rate (15 deg/h) even under motion at hundreds m/s and is multiplied by the vector β_y with small absolute magnitude. Therefore, for the impulse drift due to gyroscope data delay in a fast maneuver, the first term of (8) can be neglected, and the equation is simplified to

$$\dot\beta_y^\tau = \nu_y^\tau. \quad (9)$$

Rejecting $\hat\omega'_y\beta_y^\tau$ is tantamount to the assumption of the trihedral y stationarity, which is true over the time interval when its attitude changes slightly.

Now we qualitatively describe the effect of gyroscope impulse drifts on the navigation errors. Components ν_y^τ are present in the right sides of equations for α_i and β_3 and result in fast changes in them. Then it is known [1–3] that any errors in gyroscope channels affect only the kinematic error β included in the dynamic error α: α = β + γ, where γ is the small rotation vector corresponding to the positioning error [1–3], which barely changes during the fast maneuver. Changes in β affect the terms $g\alpha_i$ in equations for the velocity dynamic errors, which cannot be neglected as the factor g is rather large. The relevant formulas are given below

$$\dot\beta_y^\tau = \nu_y^\tau,\ \beta_y^\tau = \int_0^T \nu_y^\tau(t)dt,$$
$$\delta\dot V_y = \hat\beta_y g_y = -\hat g_y\beta_y,\ \delta V_y(T) = \hat g_y \int_0^T \beta_y^\tau(t)dt. \quad (10)$$

In the expanded form:

$$\beta_1^\tau = \int_0^T \nu_1^\tau(t)dt,\ \beta_2^\tau = \int_0^T \nu_2^\tau(t)dt,$$
$$\delta V_1(T) = -g\int_0^T \beta_2^\tau(t)dt, \quad (11)$$
$$\delta V_2(T) = g\int_0^T \beta_1^\tau(t)dt,\ \ g = |g_y|.$$

Note that if it is required to accurately calculate the delay-induced navigation errors within a maneuver with a period commensurate with the Schuler period (of the order of tens of minutes and more), accelerometer and gyroscope errors for the studied trajectory should be calculated continuously using (1) and (4). Then they should be substituted to the numerically integrated error equation system (3).

The obtained approximate formulas can be helpful to describe the navigation errors due to inertial sensor data delays in fast rotations during laboratory experiments or in short maneuvers.

Now we consider in more detail SINS fast rotations about the fixed axes with stops at some positions typical for laboratory experiments. Out of these trajectories we select those, where the delays lead to considerable navigation errors.

EFFECT OF ACCELEROMETER DATA DELAYS ON NAVIGATION ERRORS IN LABORATORY EXPERIMENTS

As is known, the measurements of accelerometer unit are recalculated to some point – the measurement center. For the rate tables, the rate and acceleration of this point are commonly rather small, and the accelerometer measurements are dominated by the specific gravity force g. In this approximation the point is considered fixed, and SINS angular rotations are made about it. Based on this assumption, we obtain the analytical expressions explaining the experimental observations associated with inertial sensor data delay, and make the numerical estimates.

With the fixed measurement center and no instrumental errors, the projections of vector g measured by the accelerometer unit are given by f_p =

$D_{px}g_x$, $g_x = [0 \;\; 0 \;\; g]^T$ = const, where D_{px} is the attitude matrix of SINS trihedral p relative to the reference frame x. The last formula takes into account that in the geographical trihedral the vector g is codirectional with the vertical – third – axis and that the accelerometer measures the projection of g with inverse sign. Therefore, $\dot{f}_p = \dot{D}_{px}g_x$.

For the pair of moving trihedrals Poisson equations $\dot{D}_{px} = \hat{\omega}_x D_{xp} - D_{xp}\hat{\omega}_p$ are true, where the term $\hat{\omega}_x D_{xp}$ can be neglected to calculate $\dot{f}_p$ over a short time period: for the rotations $|\omega_p| \sim 1$ s^{-1}, and $|\omega_x| \sim 5\cdot10^{-5}$ s^{-1}, i.e., approximately equal to the Earth's angular rate.

In this approximation,

$$\dot{D}_{px} = \dot{D}_{xp}^T \approx -(D_{xp}\hat{\omega}_p)^T = \hat{\omega}_p D_{px}$$

and

$$\begin{aligned}\Delta f_z^\tau &= -D'_{zp}T^a\dot{f}_p \approx -D_{xp}T^a\dot{f}_p = \\ &= -D_{xp}T^a\dot{D}_{px}g_x = -D_{xp}T^a\hat{\omega}_p D_{px}g_x\end{aligned}. \quad (12)$$

Note that in (12) D'_{pz}, $\hat{\omega}'_p$, g'_y calculated by SINS navigation algorithm can be used instead of the exact parameter values. The difference from the precise formula (12) in this case has the second order of smallness, which can be neglected in linear approximation.

Consider an important case when the accelerometer measurements are shifted with respect to gyroscope measurements by the same time τ^a for each axis. Then $T^a = \tau^a E$ and

$$\Delta f_x^\tau = -D_{xp}T^a\hat{\omega}_p D_{px}g_x = -\tau^a D_{xp}\hat{\omega}_p D_{px}g_x.$$

It is known [25, 28] that $D_{xp}\hat{\omega}_p D_{px} = [\hat{\omega}_p]_x$, where $[\hat{\omega}_p]_x$ is the operator of the trihedral p angular rate ω_p projected on trihedral x, which is similar to recalculation of the vector $D_{xp}\omega_p = [\omega_p]_x$. Here $[\hat{\omega}_p]_x$ denotes the operator $\hat{\omega}_p$ of trihedral p angular rate, set in the other trihedral x.

If the frames x and p coincide, $[\hat{\omega}_p]_p = \hat{\omega}_p$.

From the formula for Δf_x^τ and equality $[\hat{\omega}_p]_x g_x = -[\omega_p]_x \times g_x$ it follows that

$$\Delta f_x^\tau = \tau^a [\omega_p]_x \times g_x. \quad (13)$$

If the maneuver time is small as compared to the Schuler period, it leads to accumulation of the velocity error dynamic component (7):

$$\delta V_y = \int_0^T \Delta f_x^\tau(t)dt = \tau^a\left(\int_0^T [\omega_p]_x(t)dt\right)\times g_x. \quad (14)$$

Denote

$$I = \int_0^T [\omega_p]_x(t)dt = \int_0^T D_{xp}(t)\omega_p(t)dt = [I_1, I_2, I_3]^T.$$

Then

$$\delta V_y = \tau^a I \times g_x = g\tau^a \begin{bmatrix} I_2 & -I_1 & 0\end{bmatrix}^T. \quad (15)$$

The formula (12) allows studying the influence of arbitrary constant delays on accelerometer data.

The formula is lengthy, so generally it is rational to conduct numerical calculations. With the same delays in all three axes, formulas (12) are significantly simplified to (15), which is also convenient for analytical estimates.

ESTIMATING THE DELAYS IN ACCELEROMETER CHANNEL DURING SINS ROTATION ABOUT THE HORIZONTAL AXIS

Experimental estimation of delays in accelerometer channel is of practical interest. Consider some scenarios of these experiments. Suppose that the gyroscope channel is ideal, and data in accelerometer channel come with a constant delay τ same for all three axes. Consider SINS rotation about the sensitivity axis located in horizontal plane. Let a roll rotation about the axis x_2 oriented to the North (Fig. 1) be conducted, and at initial time $t_0 = 0$ the angles $\psi(0) = \theta(0) = \gamma(0) = 0$, and at time $t = T$ $\gamma = \gamma(T)$.

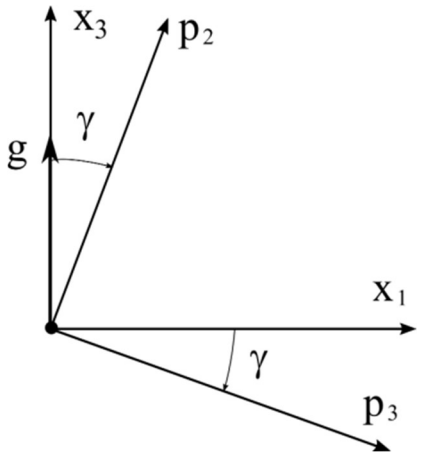

Fig. 1. SINS roll rotation: attitude of SINS and reference axes and the measured gravity force vector g.

From (12) and (14) we obtain

$$[\omega_p]_x = \begin{bmatrix} 0 & \dot\gamma & 0 \end{bmatrix}^T,\ \Delta f_z^\tau = g\tau^a,\ I_1 = 0,$$

$$I_2 = \int_0^T \dot\gamma(t)dt = I_\gamma(T),$$

$$\delta V_x(T) = g\tau^a \begin{bmatrix} I_\gamma(T) & 0 & 0 \end{bmatrix}^T.$$

It should be mentioned that $I_\gamma(T) \neq \gamma(T)$: at each rotation by 2π, 2π is added to I_γ, and the roll angle γ returns to its initial zero value.

To estimate the delay τ^a it is convenient to use SINS rotation by 2π or by the integer number of rotations $2\pi n$, which is easily realizable at any test bench. Each rotation by 2π leads to error accumulation $\delta V_1 = 2\pi g\tau^a$. With $\tau^a = 1$ ms we obtain $\delta V_1 = 0.062$ m/s. For a rotation with a constant rate the dependence of $\delta V_1(t)$ over a short time interval is presented in Fig. 2. The solution has been obtained by integrating the error equations with zero initial conditions over 100 s.

It follows from the above that delays in accelerometer channel critically degrade SINS accuracy during intensive maneuvering. For example, when an aircraft makes multiple roll or loop maneuvers, the errors will accumulate in multiples of the number of maneuvers, if the axes of these rotations have approximately the same orientation in geographical axes. This error accumulation during rotations in one direction can be used in laboratory experiments to more accurately estimate the delays.

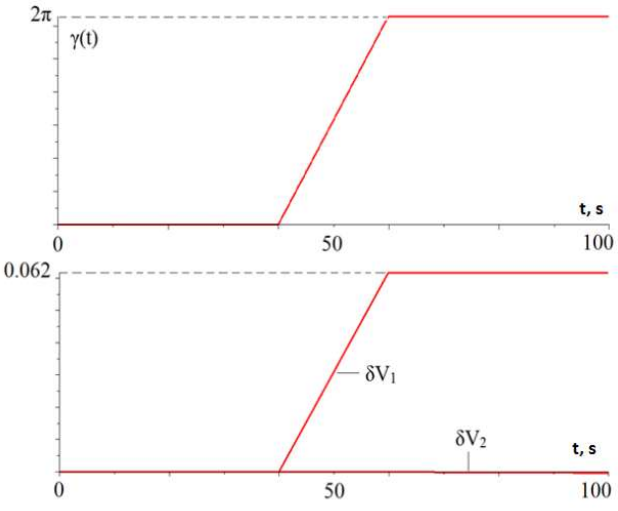

Fig. 2. Roll rotation by 2π with constant rate and the relevant linear velocity error.

Along with the delays, SINS navigation errors are influenced by the other factors including first of all sensor instrumental errors and accelerometer lever arm effect. They should be taken into consideration, and if they are significant, distinguish between the errors due to accelerometer proof mass misalignments, instrumental errors, and delays.

Consider for example the above rotation about a fixed axis by 2π under instrumental errors described with a widespread model of SINS constant instrumental errors [1–3]:

$$f_p' = (E + \Gamma)f_p + \Delta f_p,\ \omega_p' = (E + \Theta)\omega_p + \nu_p,$$

where f_p' is the specific force measured by the accelerometers, f_p is its physical value;

Γ is the matrix composed of the scale factor errors (on the main diagonal) and misalignments (nonorthogonalities) of sensitivity axes (off the diagonal);

Δf_p is accelerometer bias vector;

ω_p' is the angular rate measured by the gyroscopes, ω_p is its physical value;

Θ is the matrix of scale factor errors and misalignments, similar to Γ;

ν_p is the gyroscope drift (bias) vector.

As is known, constant projections of overall accelerometer biases on the horizontal plane and gyroscope drifts on eastern axis are compensated during SINS initial alignment. In this case SINS alignment errors α_1, α_2, β_3 compensate the instrumental errors with the projections of specific gravity force g and Earth's angular rate u. Here, [1–3]

$$\alpha_1 = -\frac{\Delta f_2}{g},\ \alpha_2 = -\frac{\Delta f_1}{g},\ \beta_3 = \frac{\nu_1}{u\cos\varphi'(0)} - \frac{\Delta f_1}{g}\mathrm{tg}\varphi'(0).$$

As a rule, SINS reference trihedral after alignment is aligned with the cardinal directions, then index 1 corresponds to the eastern direction E, and index 2, to the northern direction N. If these conditions are met, SINS has the errors consistent with the northern drift ν_2. If the compensation condition is violated, for example when SINS is turned to the other angular position, immediately after the turn the navigation errors increase.

Note that after rotation by 2π about an axis fixed relative to the Earth, the compensation condition for gyroscope drifts, accelerometer biases, axis nonorthogonalities, and scale factor errors is still satisfied. The compensation condition for them is only violated during the rotation. However, if the maneuver period is much shorter than the Schuler period and SINS has been calibrated, the navigation

errors due to these instrumental errors will change slightly during the rotation.

Consider how the remaining instrumental errors affect the navigation solution during 2π rotation. Gyroscope scale factor errors during the rotation result in accumulation of attitude errors α_i. It follows from the error equation system (3) that the errors α_i accumulated during the maneuver cause the velocity error $\delta V_i(t)$ proportional to $\sin\omega_0 t$ at the initial period, where ω_0 is the Schuler frequency. This component of vector $\delta V_i(t)$ differs from the stepwise change of δV_i during the rotation due to the delay, and therefore can be distinguished from it.

Now we demonstrate that gyroscope sensitivity axes misalignments lead to the drifts in the right part of (3) with zero mean in geographical axes when any gyroscope axis is rotated by 2π. Let the trihedrals x and p coincide at the initial time point and the axis is rotated about some fixed axis with the direction unit vector e by angle φ. Since the axis unit vector e is fixed, and the trihedrals x and p coincide at the initial time point, $e_x = e_p = \text{const}$. Matrix D_{xp} is expressed with the formula [28]

$$D_{xp} = E\cos\varphi - \hat{e}\sin\varphi + (1-\cos\varphi)ee^T .$$

Here, $\omega_p = \dot{\varphi}e$, $\nu_p = \Theta\omega_p = \dot{\varphi}\Theta e$ and

$$\nu_x = D_{xp}\nu_p = \left[E\cos\varphi - \hat{e}\sin\varphi + (1-\cos\varphi)ee^T\right]\dot{\varphi}\Theta e .$$

Integrating this formula over the 2π rotation time T with account for averaging

$$\int_0^T \sin\varphi\dot{\varphi}dt = \int_0^{2\pi}\sin\varphi d\varphi = \int_0^T \cos\varphi\dot{\varphi}dt = \int_0^{2\pi}\cos\varphi d\varphi = 0$$

yields

$$\beta_x = \int_0^T \nu_x dt = 2\pi e(e^T\Theta e) .$$

The given formula describes the kinematic error accumulated during the rotation about an arbitrary fixed axis due to the gyroscope scale factor errors or misalignments forming the matrix Θ. During the rotation about any sensitivity axis, the vector e has the only non-zero component equal to one. If it is at the position of i, then $e^T\Theta e = \Theta_{ii}$. If the matrix Θ includes the misalignments only, then $\Theta_{ii} = 0$, $\Theta_{i\neq j} \neq 0$, $e^T\Theta e = 0$, which was to be shown.

The assumption that the trihedrals x and p coincide at $t = 0$ does not limit the generality: at initial arbitrary orientation of x and p the right part of $\nu_x = D_{xp}\nu_p$ is multiplied at the left by the constant initial attitude matrix of x and p, which does not affect the obtained result.

Emphasize that in the laboratory experiment the accelerometers measure the projections of g. However, when the SINS onboard an object is moving, it is subject to accelerations exceeding manifold g. During the maneuver the measured acceleration (specific force) is not any more aligned with the vertical axis of the reference trihedral x. Therefore, to calculate the navigation errors, numerical integration of (3) should be conducted rather than applying (14) and (15). It follows from (1) that under intensive maneuvering with large and fast changing accelerations, the delay-induced accelerometer errors and, correspondingly, SINS navigation errors are expected to grow.

Velocity errors during the rotation with different accelerometer delays are derived from (12). For the rotation about the first SINS axis p_1 considered above, and $\tau_2 \neq \tau_3$ for the axes p_2 and p_3, the following is substituted to (12):

$$D_{xp} = \begin{bmatrix} 0 & \sin\gamma & \cos\gamma \\ 1 & 0 & 0 \\ 0 & \cos\gamma & -\sin\gamma \end{bmatrix},\ T^a = \operatorname{diag}[0,\tau_2,\tau_3],$$
$$\hat{\omega}_p = \begin{bmatrix} 0 & 0 & 0 \\ 0 & 0 & \dot{\gamma} \\ 0 & -\dot{\gamma} & 0 \end{bmatrix},\ g_x = \begin{bmatrix} 0 \\ 0 \\ g \end{bmatrix}. \qquad (16)$$

Integrating the right part of (12) yields

$$\delta V_1 = \frac{\tau_2 - \tau_3}{2} g\sin 2\gamma - I_\gamma g\frac{\tau_3 + \tau_2}{2} . \qquad (17)$$

Therefore, over a complete rotation by 2π the velocity error proportional to the average value of $(\tau_3 + \tau_2)/2$ is accumulated. In rotations by arbitrary angles, the velocity error is no longer proportional to the rotation angle, however, the function $\sin\gamma$ is zeroed at rotations by angles multiple of π/2, and the difference $\tau_2 - \tau_3$ cannot be detected by δV_1.

Repeating the experiments with 2π rotations for all three sensitivity axes, which are initially set to the horizontal plane along the northern direction, helps to estimate the delay sums:

$$\tau_1 + \tau_2 = \overline{\tau}_1,\ \tau_2 + \tau_3 = \overline{\tau}_2,\ \tau_3 + \tau_1 = \overline{\tau}_3 .$$

In the right part of equations, the symbols $\overline{\tau}_i$ denote the estimates following from (17): $\overline{\tau}_k = -(\pi g)^{-1}\delta V_1^k(T)$, where $\delta V_1^k(T)$ is the accumulation of velocity error in the k-th experiment. Solv-

ing the given equation system with respect to τ_i, we obtain the estimates of the delays:

$$\tau_1 = \frac{1}{2}\left(\overline{\tau}_1 + \overline{\tau}_3 - \overline{\tau}_2\right),\ \tau_2 = \frac{1}{2}\left(\overline{\tau}_2 + \overline{\tau}_1 - \overline{\tau}_3\right),$$
$$\tau_3 = \frac{1}{2}\left(\overline{\tau}_3 + \overline{\tau}_2 - \overline{\tau}_1\right).$$

Negative estimates mean that accelerometer data are ahead of gyroscope data.

Therefore, SINS rotations about the axes of the SINS trihedral, which are close to the inertial sensor sensitivity axes, with further fixation cause the stepwise accumulation of the velocity error due to accelerometer data delays. The simplest expressions for these errors are obtained if the rotation axes are fixed relative to the Earth and are aligned with a cardinal direction, such as the North. We propose a three-rotation scenario for estimating the accelerometer delays in all three axes.

EFFECTS OF GYROSCOPE DATA DELAYS AND THEIR DETECTION IN LABORATORY EXPERIMENTS

We use the Eqs. (6) and (9) assuming that the maneuver is short compared to Schuler period:

$$\nu_z^\tau = D'_{zp} T^g \dot{\omega}_p \approx \nu_x^\tau = D_{xp} T^g \dot{\omega}_p,\ \dot{\beta}_x^\tau = D_{xp} T^g \dot{\omega}_p. \quad (18)$$

Integrate the equation for β_x^τ by parts assuming that $\beta_x^\tau(0) = 0$:

$$\beta_x^\tau(t) = \int_0^t D_{xp}(\tau) T^g \dot{\omega}_p(\tau) d\tau = \int_0^t D_{xp}(\tau) T^g d\omega_p(\tau) = \quad (19)$$
$$= D_{xp}(\tau) T^g \omega_p(\tau)\Big|_0^t - \int_0^t \dot{D}_{xp}(\tau) T^g \omega_p(\tau) d\tau.$$

During the maneuver the matrix D_{xp} changes mostly due to fast motion of trihedral p in inertial space described by Poisson equations $\dot{D}_{xp} = -D_{xp}\hat{\omega}_p$. Therefore,

$$\beta_x^\tau(t) = D_{xp}(\tau) T^g \omega_p(\tau)\Big|_0^t + \int_0^t D_{xp}(\tau)\hat{\omega}_p(\tau) T^g \omega_p(\tau) d\tau. \quad (20)$$

Hence it follows that if the delays in all three channels are identical and equal to τ^g, then $T^g = \tau^g E$ and $\hat{\omega}_p T^g \omega_p = \tau^g \hat{\omega}_p \omega_p = 0$. If the motion starts and ends with a quiescent state relative to the Earth, then $\omega_p(0) = \omega_p(t) = 0$ and $\beta_x^\tau(t) = 0$. During the motion

$$\beta_x^\tau(t) = D_{xp}(t) T^g \omega_p(t) = \tau^g [\omega_p(t)]_x, \quad (21)$$

which suggests the following interpretation: $\tau^g\omega$ in linear approximation is equal to the Euler rotation vector [25, 28] of the body with angular rate ω_p within the delay time τ^g.

If $T^g \neq \tau^g E$, then $D_{xp}\hat{\omega}_p T^g \omega_p \neq 0$ and the attitude error may accumulate at the stop after the turn.

Note that the arbitrary matrix T^g allows the representation below

$$T^g = \tau_1 E + \mathrm{diag}\left[0, \tau_2 - \tau_1, \tau_3 - \tau_1\right] = \tau_1 E + \delta T^g, \quad (22)$$

distinguishing between the delays relative to the accelerometers τ_1 and mutual delays of measurement channels characterized by the matrix δT^g. The first axis for the τ_1 measurement was selected conditionally and can be substituted with any other. As a result, we obtain the following expression:

$$\beta_x^\tau(t) = \tau_1 D_{xp}(\tau)\omega_p(\tau)\Big|_0^t + \int_0^t D_{xp}(\tau)\hat{\omega}_p(\tau)\delta T^g \omega_p(\tau) d\tau. \quad (23)$$

Consider the effects of SINS errors under delays of gyroscope data relative to the accelerometers and between the gyroscope axes separately.

Delay of Gyroscope Triad Data Relative to the Accelerometer Triad

If the motion starts from the quiescent state, then it follows from (10), (11), and (21) that

$$\beta_x^\tau(t) = \tau^g [\omega_p(t)]_x,$$
$$\delta V_y(T) = -\hat{g}_x \int_0^T \beta_x^\tau(t) dt = -\tau^g \hat{g}_x \int_0^T [\omega_p(t)]_x dt. \quad (24)$$

Denoting $I = \int_0^T [\omega_p(t)]_x dt$, we obtain

$$\delta V_y(\mathrm{T}) = \tau^g I \times g_x = g\tau^g \left[-I_2 \quad I_1 \quad 0\right]^T, \quad (25)$$

which coincides with (15), if τ^a is substituted with $(-\tau^g)$. Therefore, rotation about the horizontal axis coinciding with one of sensitivity axes results in the error δV_y, the same as under accelerometer channel delay relative to the gyroscopes, but with the opposite sign.

It should be emphasized that, unlike the accelerometer delays, gyroscope delays induce the accumulation of navigation errors due to the errors in g projections at the turns rather than the specific force measured by the accelerometers. However, in ground-based experiments during the turns, when

the acceleration of the accelerometer unit measurement center is negligibly small compared to g, $f \approx -g$, which conditions the coincidence of (15) and (25) accurate to the sign.

It should be mentioned that (25) would be true not only for laboratory experiment with slow-moving accelerometer measurement center, but also for arbitrary space maneuvering.

Data Delays between Gyroscope Axes

With different delays in gyroscope sensitivity axes, the integral term in (23) will be different from zero. In some maneuvers, the related attitude errors may accumulate and serve as the main reason for increased errors in SINS inertial data.

Further we describe some motions that can be used to identify the delays and can be reproduced in the laboratory tests. Some of these motions were determined in [11–16]. The results described in these references may be obtained using the formulas above.

Assume that the angular rate of SINS trihedral p is determined by its motion relative to the geographical trihedral x, which can be considered fixed within an experiment rather short compared to the Schuler period.

Substitute $\tau_2 - \tau_1 \mapsto \tau_2,\ \tau_3 - \tau_1 \mapsto \tau_3$ in (22), then

$$T^g = \mathrm{diag}[0\ \ \tau_2\ \ \tau_3]. \tag{26}$$

One of the motions affecting the mutual delays in gyroscope channels and easily reproducible on the test benches is harmonic oscillations about the Earth-bound horizontal axis non-collinear to one of the gyro sensitivity axes.

To obtain compact formulas, it is convenient to direct the oscillation axis to the North along the axis x_2° (here and below x° denotes a trihedral with the axes aligned with the cardinal directions) according to Fig. 3.

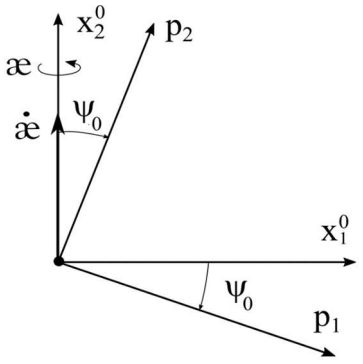

Fig. 3. Oscillations about a horizontal axis directed to the North.

Assume that at initial time the heading, pitch, and roll angles [1–3] are respectively $\psi(0) = \psi_0$, $\theta(0) = \gamma(0) = 0$, and the angle κ sets the SINS rotation relative to x_2° and $\kappa(0) = 0$. The formulas for SINS trihedral p with the axes aligned with the axes x° under $\psi(0) = \theta(0) = \gamma(0) = 0$ are given below.

For this motion,

$$\dot\beta_x^\tau = \nu_{x^\circ} = D_{x^\circ p}\nu_p = D_{x^\circ p}T^g\dot\omega_p,$$
$$D_{x^\circ p} = \begin{bmatrix} \cos\psi_0\cos\kappa & \sin\psi_0\cos\kappa & \sin\kappa \\ -\sin\psi_0 & \cos\kappa & 0 \\ -\cos\psi_0\sin\kappa & -\sin\psi_0\sin\kappa & \cos\kappa \end{bmatrix},$$
$$\dot\omega_p = \ddot\kappa \begin{bmatrix} -\sin\psi_0 \\ \cos\psi_0 \\ 0 \end{bmatrix}, \tag{27}$$
$$\nu_{x^\circ} = \ddot\kappa\tau_2\cos\psi_0 \begin{bmatrix} \sin\psi_0\cos\kappa \\ \cos\psi_0 \\ -\sin\psi_0\sin\kappa \end{bmatrix}.$$

For the case of harmonic oscillations simulated on automated test beds, $\kappa = \kappa_0\sin\omega t$, then

$$\nu_{x^\circ} = \kappa_0\tau_2\omega^2 \times$$
$$\times\cos\psi_0 \begin{bmatrix} -\sin\psi_0\cos(\kappa_0\sin\omega t)\sin\omega t \\ \cos\psi_0\sin\omega t \\ \sin\psi_0\sin(\kappa_0\sin\omega t)\sin\omega t \end{bmatrix}. \tag{28}$$

Since the oscillation period is much shorter than the Schuler period, SINS errors are mostly affected by the average values of the right part of (28). The first two components of the vector ν_{x° are odd functions, consequently, having zero mean. In [11] A.V. Kozlov determined that the mean of the third component is accurately calculated for an arbitrary amplitude κ_0:

$$\left\langle \nu_{x^\circ} \right\rangle = \frac{1}{2}\kappa_0\tau_2\omega^2\sin 2\psi_0 J_1(\kappa_0)\begin{bmatrix}0 & 0 & 1\end{bmatrix}^T, \tag{29}$$

where $J_1(\kappa_0) = \frac{1}{\pi}\int_0^\pi \sin x\sin(\kappa_0\sin x)dx$ is the Bessel function of the first kind. For oscillations with rather small amplitude, $\kappa_0 \ll 1$ (in rad) and

$$\left\langle \nu_{x^\circ} \right\rangle = \frac{1}{4}\kappa_0^2\tau_2\omega^2\sin 2\psi_0\begin{bmatrix}0 & 0 & 1\end{bmatrix}^T. \tag{30}$$

Thus, under non-synchronous data readout from the gyroscopes, oscillations can produce non-averaged drifts in the reference trihedral and the right part of the error equation. Maximal drift is ob-

served if the oscillations axis makes angles $\psi_0 = \pm\pi/4$ with the gyroscope sensitivity axes.

Denoting $\nu = \left|\left\langle \nu_{x^\circ} \right\rangle\right|$, from (30) we obtain

$$\kappa_0 = \frac{2}{\omega}\sqrt{\frac{\nu}{\tau_2}} = \frac{1}{\pi f}\sqrt{\frac{\nu}{\tau_2}}, \qquad (31)$$

where f is the frequency corresponding to the angular frequency ω in Hz. This formula is convenient for numerical estimates. Take the drift ν = 0.01 deg/h typical of a 1 nm/h SINS, and assume that $\tau_2 = 10^{-6}$ s. Then (31) gives the dependence $\kappa_0(f)$ presented in Fig. 4.

Mention that with f = 0.5 Hz κ_0 = 8° and these oscillations can be reproduced at the rate table, and with f = 100 Hz κ_0 = 2.4′, which is realizable during SINS vibration tests or its installation on high-vibration objects.

Precession motion with precession and self-rotation frequency ratio 1:2 is considered in [13], where drift with nonzero mean in geographical frame also occurs due to gyroscope data delays. Reproducing this motion in experimental conditions requires a three degree-of-freedom rate table.

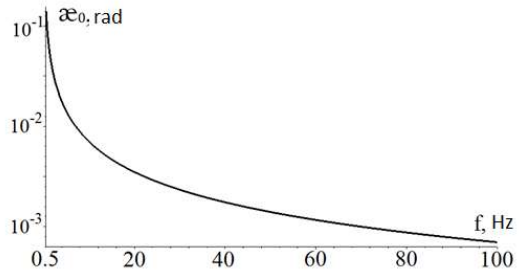

Fig. 4. Dependence $\kappa_0(f)$ [rad] in log scale for ν = 0.01 deg/h, $\tau_2 = 10^{-6}$.

This motion can be used to study how detuning of rotation frequencies impacts the drifts due to gyroscope data delay. It turns out that even a minor detuning significantly lowers the drift since it no longer contains the constant non-averaged component. The reader is referred to [13] for details. Another type of motion with frequency ratio 1:2 but without monotonous rotations is described in [11].

The effect of frequency detuning on the drift suggests that in general case the gyroscope data delays influence SINS errors to a much lower degree than under special motions considered above. The delays are expected to be more influential under some cyclical motions.

The formula (30) can be applied to estimate the data delays between gyroscopes. More complicated techniques are needed to distinguish between the navigation errors due to data delays between the gyroscopes and instrumental errors if required. Some of these techniques are discussed in [11].

RECOMMENDATIONS ON REDUCING THE DELAY-INDUCED ERRORS

Inertial sensor data delays critically affect SINS errors in some maneuvers. Therefore, synchronization of SINS inertial sensor measurements, first at the hardware level, is of primary importance during processing. However, if due to some reasons cannot be eliminated, their effect can be mitigated algorithmically.

To compensate the gyroscope data delay, the kinematic equations

$$\dot{\beta}_y^\tau = \hat{\omega}'_y\beta_y^\tau + \nu_y^\tau, \;\; \beta_y^\tau(0) = 0, \; \nu_y^\tau = D'_{zp}T^g\dot{\omega}_p$$

can be integrated.

The right part of equations is calculated by the parameters determined by SINS algorithms, and matrix T^g can be estimated using the method described above, for example, during the oscillation experiment. The value β_y^τ (see the section Effects of Gyroscope Data Delays and Their Detection in Laboratory Experiments) can be used to correct the matrix D'_{zp} or added to the right part of equations $\dot{V}'_y = (2\hat{u}'_y + \hat{\Omega}'_y)V'_y + g'_y + f'_z$ for the horizontal components V'_1, V'_2 of vector V'_y as a correction $\hat{\beta}_y^\tau g'_y$ calculated by (10). Note that integrating the equation for β_y^τ smoothens the noise ν_y^τ in its right part.

The errors due to accelerometer channel data delays are described by (1). However, its applicability for delay compensation depends of many factors: accelerometer noise, computation frequency, delay values, features of trajectories, and therefore requires additional research for each type of SINS and its operation conditions.

CONCLUSIONS

The paper analyzes the influence of data delays in the channels of SINS inertial sensors – gyroscopes and accelerometers – on SINS navigation errors. Different combinations of delays in groups

of one-type sensors and between different sensors have been studied. Formulas for the biases or drifts due to time delays in the right part of SINS error equation system are presented for each case.

Qualitative analysis of SINS navigation errors dependency on the delays has been conducted for typical short maneuvers as compared to the Schuler period. Analytical expressions have been obtained for estimating the delay effect under arbitrary angular motion in laboratory experiments, with the measurement center of accelerometer unit considered to be fixed. This, in its turn, allows developing test scenarios for detecting the delays.

Accelerometer data delays are shown to result in the overall accelerometer biases in the error equations, proportional to the derivatives of the sensor data.

Delays of gyroscope triad data (identical for all three axes) relative to the accelerometers also condition the overall accelerometer biases, however, they are proportional to *g* projections and are insensitive to the accelerometer measurements.

Microsecond-order data delays between the gyroscopes in different axes lead to significant overall drifts under specific types of motions reproduced by the test bench or caused by oscillations or vibrations. Test scenarios that can be used to detect and estimate the delays have been considered, and recommendations on their algorithmic compensation are provided.

FUNDING

This work was supported by ongoing institutional funding. No additional grants to carry out or direct this particular research were obtained.

CONFLICT OF INTEREST

The authors of this work declare that they have no conflicts of interest.

REFERENCES

1. Golovan, A.A. and Parusnikov, N.A., *Matematicheskie osnovy navigatsionnykh sistem.* Part 1. *Matematicheskie modeli inertsial'noi navigatsii* (Mathematical Foundations of Navigation Systems. Part 1. Mathematical Models of Inertial Navigation), Moscow: MAKS Press, 2011, third ed.
2. Vavilova, N.B., Golovan, A.A., and Parusnikov, N.A., *Matematicheskie osnovy inertsial'nykh navigatsionnykh system* (Mathematical Foundations of Inertial Navigation Systems), Moscow: Moscow State University, 2020.
3. Vavilova, N.B., Golovan, A.A., and Parusnikov, N.A., *Kratkii kurs teorii inertsial'noi navigatsii* (A Short Course in Inertial Navigation Theory), Moscow: ICP RAS, 2022.
4. Andreev, V.D., *Teoriya inertsial'noi navigatsii. Avtonomnye sistemy* (Theory of Inertial Navigation. Autonomous Systems), Moscow: Nauka, 1966.
5. Emel'yantsev, G.I. and Stepanov, A.P., *Integrirovannye inertsial'no-sputnikovye sistemy orientatsii i navigatsii* (Integrated INS/GNSS Orientation and Navigation Systems), St. Petersburg: Concern CSRI Elektropribor, JSC, 2016.
6. Panov, A.P., *Matematicheskie osnovy teorii inertsial'noi orientatsii* (Mathematical Foundations of the Theory of Inertial Attitude Determination), Kiev: Naukova Dumka, 1995.
7. Branets, V.N. and Shmyglevskii, I.P., *Vvedenie v teoriyu besplatformennykh inertsial'nykh navigatsionnykh sistem* (Introduction to the Theory of Strapdown Inertial Navigation Systems), Moscow: Nauka, 1992.
8. Savage, P.G., *Strapdown Analytics*, Maple Plain, Minessota: Strapdown Associates, Inc., 2000.
9. Litmanovich, Yu.A., Use of angular rate multiple integrals as input signals for strapdown attitude algorithms, *Symposium Gyro Technology*, Stuttgart, Germany, 1997.
10. Marc, J.G. and Tazartes, D.A., Application of coning algorithms to frequency shaped gyro data, *6th St. Petersburg International Conference on Integrated Navigation Systems*, RTO Meeting Proceedings, 43, 1999.
11. Kozlov, A.V., Kapralov, F.S., and Fomichev, A.V., Calibration of a timing skew between gyroscope measurements in a strapdown inertial navigation system, *26th St. Petersburg International Conference on Integrated Navigation Systems*, 2019. https://doi.org/10.23919/ICINS.2019.8769417
12. Kukhtevich, S.E., Rafel'son, V.F., and Fomichev, A.V., On SINS errors due to timing skews of angular rate and linear acceleration measurement channels and the geometry of accelerometer unit, *Trudy MIEA. Navigatsiya i upravlenie letatel'nymi apparatami,* 2011, no. 3, pp. 86–65.
13. Bogdanov, O.N. and Fomichev, A.V., Effect of delays in rate sensor channels on the accuracy of navigation solution of strapdown inertial navigation system, *Gyroscopy and Navigation,* 2018, vol. 9, no. 3. https://doi.org/10.1134/S2075108718030033
14. Kuznetsov, A.G. and Fomichev, A.V., On computational drift caused by angular rate sensors desynchronization under vibration influence on SINS, *Navigatsiya i upravlenie letatel'nymi apparatami*, 2023, no. 42, pp. 9–28.
15. Slysar, V.M., Relevant issues of SINS attitude determination algorithms design. Part 3. Algorithm analysis and synthesis with account for the gyroscope frequency characteristics, *Giroskopiya i Navigatsiya*, 2006, no. 4 (55).
16. Zlatkin, Y.M., Kalnoguz, A.N., Voronchenko, V.G. et al., Laser SINS for Cyclone-4 launch vehicle, *Gyroscopy and Navigation,* 2013, vol. 4, no. 3. https://doi.org/10.1134/S2075108713030085

17. Klimkovich, B.V. and Tolochko, A.M., Determination of time delays in measurement channels during SINS calibration in inertial mode, *Gyroscopy and Navigation*, 2016, vol. 7, no. 2. https://doi.org/10.1134/S2075108716020048
18. Jinlong Xing, Gongliu Yang, and Tijing Cai, Modeling and calibration for dithering of MDRLG and time-delay of accelerometer in SINS, *Sensors*, 2022, 22, 278. https://doi.org/10.3390/s22010278
19. Vavilova, N.B., Golovan A.A., Kozlov A.V., Papusha I.A., Zorina, O.A, Izmailov, E.A., Kukhtevich, S.E., and Fomichev, A.V., INS/GNSS integration with compensated data synchronization errors and displacement of GNSS antenna. Experience of practical realization, *Gyroscopy and Navigation*, 2021, vol. 13, no. 4, pp. 236-246. https://doi.org/10.1134/S207510872103007X
20. Weina Chen, Zhong Yang, Shanshan Gu, Yizhi Wang, and Yujuan Tan, Adaptive transfer alignment based on observability analysis for airborne pod strapdown inertial navigation system, *Nature Scientific Reports*, 2022, 12, 946. https://doi.org/10.1038/s41598-021-04732-4
21. Weiwei Lyu and Xianghong Cheng, A novel adaptive H∞ filtering method with delay compensation for the transfer alignment of strapdown inertial navigation systems, *Sensors*, 2017, vol. 17, 2753. https://doi.org/10.3390/s17122753
22. Lee, K., and Johnson, E.N., Latency compensated visual-inertial odometry agile autonomous flight, *Sensors*, 2020, vol. 20, 2209. https://doi.org/10.3390/s20082209
23. Bo Xu, Xiaoyu Wang, Jiao Zhang, and Razzaqi, A.A., Maximum correntropy delay Kalman filter for SINS/USBL integrated navigation, *ISA Transactions,* 2021, vol. 117 (9). https://doi.org/10.1016/j.isatra.2021.01.0550019-0578
24. Kozlov, A. and Kapralov, F., Angular misalignment calibration for dual-antenna GNSS/IMU navigation sensor, *Sensors*, 2023, vol. 23, 77. https://doi.org/10.3390/s23010077
25. Zhuravlev, V.F., *Osnovy teoreticheskoi mekhaniki* (Foundations of Theoretical Mechanics), Moscow: Fizmatlit, 2001.
26. Markeev, A.P., *Teoreticheskya mekhanika* (Theoretical Mechanics), Moscow: IKI, 2024.
27. Bolotin, S.V., Karapetyan, A.V., Kugushev, E.I., and Treshchev, D.V., Teoreticheskaya mekhanika (Theoretical Mechanics), Moscow: Academia, 2010.
28. Fomichev, A.V., *Kinematika tochki i tverdogo tela* (Kinematics of the Point and the Solid Body), Moscow: Moscow Institute of Physics and Technology, 2021.